Part 3

New philosophies of control and economics in distribution systems

Chapter 6

Customer modeling and pricing-mechanisms for demand response in smart electric distribution grids

Timothy M. Hansen, Robin Roche**, Siddharth Suryanarayanan†, Anthony A. Maciejewski†, Howard Jay Siegel†,‡, and Edwin K. P. Chong†*

Abstract

We describe and contrast different market mechanisms to incentivize residential electricity customers to perform demand response (DR) via load shifting of *schedulable assets*. A customer-incentive pricing (CIP) mechanism from our past research is discussed, and compared to flat-rate, time-of-use (TOU), and real-time pricing (RTP). The comparison is made using a for-profit aggregator-based residential DR approach to solve the "Smart Grid resource allocation" (SGRA) problem. The aggregator uses a heuristic framework to schedule customer assets and to determine the customer-incentive price to maximize profit. Different customer response models are proposed to emulate customer behavior in the aggregator DR program. A large-scale system consisting of 5,555 residential customer households and 56,588 schedulable assets using real pricing data over a period of 24 h is simulated and controlled using the aggregator. We show that the aggregator enacts a beneficial change on the load profile of the overall power system by reducing peak demand. Additionally, the customers who are more *flexible* with their loads, represented as a parameter in the proposed customer α-model, have a greater reduction on their electricity bill.[1]

*Electrical Engineering and Computer Science Department, South Dakota State University, Brookings, SD, USA

**IRTES, Université de Technologie de Belfort-Montbéliard, Université Bourgogne Franche-Comté, Belfort, France

†Department of Electrical and Computer Engineering, Colorado State University, Fort Collins, CO, USA

‡Department of Computer Science, Colorado State University, Fort Collins, CO, USA

[1]This chapter is an expanded version of a journal article [1]. Project codes and data sets have been made available for use through the open source BSD 3-Clause license at https://github.com/IPEMS

6.1 Customer modeling introduction

The US Energy Information Administration predicts a 24% increase in residential electricity use from a 2013 reference case to the year 2040. Additionally, since 1982 the growth in peak electricity usage has exceeded the growth in transmission capacity by almost 25% each year [2]. Given the combination of these trends, it is expected that peak energy demands will approach, and eventually exceed, the available transmission system capability (the remaining power that could be transferred from generation to consumption). A side consequence of these trends, in addition to the possibility of system outage, is more congestion on transmission lines, leading to increased locational marginal prices (LMP) – different marginal prices (price of providing the next MW of power) at different buses in the transmission network. Studies show that small and targeted reductions in peak demand can have large impacts on wholesale electricity prices [3]. As shown in Reference 2, it is unlikely that additional spending will be allocated for increasing transmission capability, leading to research in the areas of distributed generation (DG) and, in the case of this chapter, shifting or curtailing load during peak hours. Given that residential customers can account for over half of the system peak demand in summertime, such as in markets like the Electric Reliability Council of Texas (ERCOT) [4], residential demand response (DR) programs are attractive solutions for relieving the stress on the system and market. In this work, we define the term DR to be the reduction in peak demand by shifting or shedding loads in response to system or economic conditions to alleviate stress on the electric power system.

As presented in Reference 5, incentives can influence customer behavioral changes. Dynamic pricing programs are one method for accomplishing DR. These utility-offered programs, such as time-of-use (TOU) and real-time pricing (RTP), fluctuate the price of electricity throughout the day in accordance with system load levels to elicit a change in the consumption of electricity [6]. In this chapter, we introduced an additional pricing method, *customer-incentive pricing* (CIP), which provides the residential end-user an additional competitive pricing scheme for participating in a targeted DR program through an aggregator. The aggregator in this chapter is a for-profit entity in a deregulated market structure that interfaces a *DR* exchange market (DRX) and a set of customers. The aggregator uses the combination of many customer schedulable assets of the participating customers to perform large-scale load shifting. In many, if not all energy markets, there is a minimum power rating required to bid into the market (e.g., 0.1 MW in the PJM market [7]). The aggregator entity is able to enact a change on the electric power system load profile by bidding the aggregate load of customer assets into the bulk market through the DRX.

By voluntarily opting into the aggregator DR program, the customer is provided the opportunity to participate in the bulk power market. Residential customers can change electricity use to take advantage of the time-varying rates provided by the utility and aggregator to reduce their electricity bill. The challenges of an effective residential DR program are (a) the uncertainty in the time-varying price of electricity and (b) that as a customer, the benefit received from changing energy usage must exceed the inconvenience caused. To overcome these challenges and to

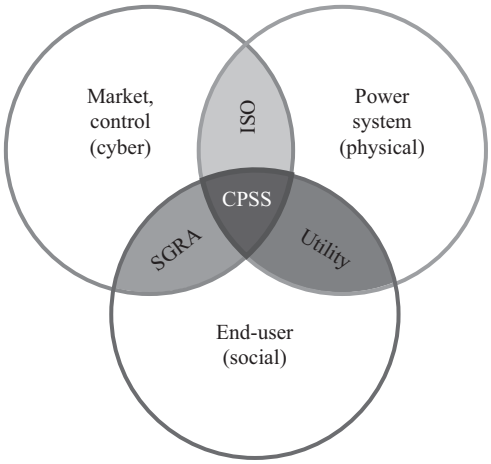

Figure 6.1 The proposed SGRA CPSS lies at the intersection between the power system network, market and controls, and end-user

maximize the benefit of dynamic pricing, we introduce the aggregator-based residential DR program, denoted Smart Grid Resource Allocation (SGRA), where given a set of participating customers with schedulable assets, subject to customer constraints (i.e., availability of customer assets and customer incentive requirements), the aggregator sets the *CIP* and *schedule of assets* to maximize profit of the aggregator while not inconveniencing the participating customer. The SGRA is formulated as a cyber-physical-social system (CPSS), as illustrated in Figure 6.1.

The proposed SGRA CPSS lies at the intersection of the *physical* electric power network, *cyber* market and control layer, and *social* residential end-users. The independent system operator (ISO) interfaces the bulk power market and physical equipment. Local utilities traditionally deliver power to end-user customers through the distribution network. The aggregator entity provides the residential end-user a path to participate in the market. The SGRA problem is solved using resource allocation methods analogous to those used in the computing discipline, where compute tasks must be allocated to machines. In general, such problems are NP-complete [8–10], so heuristic optimization is used to find *near-optimal* solutions. In this chapter, we use heuristic optimization techniques to find near-optimal solutions to the SGRA problem in a reasonable time frame to be used as a day-ahead scheduler of a large number of residential end-user assets.

According to the California Energy Commission (CEC), residential loads are not easily controlled and need to be composed of a large portfolio of assets to provide a strategic DR product [11]. The work in this chapter directly addresses the CEC DR strategies (direct DR participation with the ISO, new market and auction mechanisms, e.g., our proposed DRX, improving customer willingness to participate, and the introduction of time-variant pricing) by offering direct DR participation through

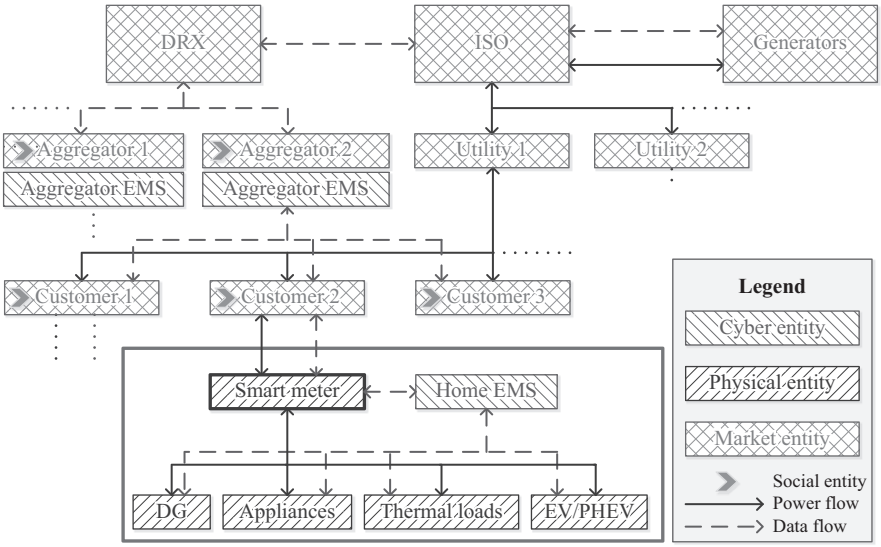

Figure 6.2 The architecture and communication for the proposed aggregator-based residential DR program CPSS, expanded from Reference 1

the customer-aggregator-DRX relationship (see Figure 6.2) and encouraging customer participation with the time-variant CIP mechanism. In this chapter, a heuristic framework is designed and implemented; and customer-behavior is emulated using a proposed α-model. To quantify the impact of the SGRA CPSS, a simulation study is conducted where the aggregator schedules over 56,000 end-user assets from 5,555 customers. Comparisons are made between different utility pricing mechanisms, namely TOU, RTP, and flat-rate.

The rest of the chapter is organized as follows. In Section 6.2.3, the aggregator-based residential DR is formally introduced in the context of CPSS. To mimic customer behavior in large simulation studies, mathematical customer behavior models are defined in Section 6.3. Section 6.4 summarizes commonly used utility pricing mechanisms. The heuristic framework and problem formulation are derived in Section 6.5. A large-scale simulation study of the SGRA problem is conducted in Section 6.6, and Section 6.7 concludes.

6.2 Aggregator-based residential demand response

6.2.1 CPSS

The proposed CPSS for the aggregator-based residential DR program is shown in Figure 6.2. The right side of the CPSS shows the power flow and market structure of the traditional electric power system. The ISO coordinates the generators in the

system (supply) and load requirements of the utilities (demand) to ensure power balance reliably and at the cheapest price. The utilities deliver the power to the end-user, in this case residential customers. Industrial and commercial end-users can also be considered in the SGRA by modeling their assets, but this is not presented in this chapter. The left-hand side of Figure 6.2 encapsulates our proposed residential DR program. The DRX is an ancillary market in a fully deregulated market structure that provides DR services to the ISO. The aggregator interfaces the DRX and the residential customer, and provides the positive attributes (e.g., load shifting, distributed storage) of the aggregated customer assets (e.g., DG, electric vehicles) to the ISO. The aggregator coordinates the use of the participating customer assets and brings the result, such as peak shaving, to the DRX for market exchange.

6.2.2 Aggregator

The aggregator is a for-profit market entity engaged in interacting with the customer and the bulk power market in a fully deregulated market structure. As shown in Figure 6.2, the aggregator is situated between the DRX and the customer. The aggregator energy management system interacts with each of the customer home energy management systems (HEMS). In this chapter, we are only considering one aggregator entity, but it is expected that several aggregators may exist within the same distribution area.

The aggregator coordinates a set of participating customers, each with a set of schedulable assets. In this chapter, we are currently only considering schedulable loads in the form of smart appliances (e.g., dishwashers, washer, dryer), but this approach could be extended to other types of assets such as DG, thermal loads (e.g., electric water heaters [12] and heating-ventilation-air-conditioning systems [13]), and electric vehicles in the form of vehicle-to-grid [14] or scheduling vehicle charging cycles [15].

The scheduling problem is proposed as a day-ahead optimization. To make decisions, the aggregator requires information about the customer loads, the forecast utility pricing, and the forecast spot market pricing (SMP) in the bulk electricity market. Using this information, the aggregator must find the *CIP* and *schedule of loads* to maximize its profit. Because it is a day-ahead optimization, there are constraints on the execution time of the optimization technique used. This time constraint and the complexity of the scheduling problem (i.e., the class of problems is, in general, NP-complete) due to the large number of customer assets leads to the use of heuristic optimization. Other objectives could be considered, such as minimizing the peak load, or considering multiple objectives in the form of a multi-objective optimization using Pareto-fronts [16]. In this chapter, we solely optimize for the aggregator profit to demonstrate that a purely economic motivation will affect the desired change of reduced system peak demand.

6.2.3 Aggregator demand response

CIP is a proposed pricing structure that the aggregator would offer all customers to allow the rescheduling of their loads. That is, instead of paying the utility company,

the customer pays the aggregator the CIP for electricity. The customer paying the CIP for electricity to the aggregator at the time the asset has been rescheduled *to* is one part of the profit of the aggregator. The sum of these payments over all customers and all rescheduling events is denoted S. The other two components to the aggregator profit are: (a) the aggregator selling a negative load to the spot market where the assets have been rescheduled *from* (denoted N), and (b) the aggregator buying spot market electricity where the assets have been rescheduled *to* (denoted B). The aggregator would, perhaps, need to enter into a leasing agreement with the utility company for the use of the distribution assets, but modeling this and other potential fixed costs are beyond the scope of this chapter.

To reschedule load, the aggregator requires information on the set of schedulable loads. These schedulable loads represent a subset of the system load. For each schedulable load i, the aggregator receives the following information on the schedulable appliances of each participating customer:

- δ_i, the runtime duration (in 15-min intervals);
- p_i, the average power rating (in kW);
- t_{i_start}, the customer scheduled start time; and
- (A_{i_start}, A_{i_dur}), a 2-tuple that represents the customer-defined availability window for load i determined by the availability window start time, A_{i_start}, and the availability window duration, A_{i_dur}.

In this chapter, we assume that the aggregator knows the exact time a load will run (i.e., from t_{i_start} for δ_i time intervals) if it is not rescheduled by the aggregator (i.e., the start time is deterministic). This could be represented as a probability distribution based on historical runtimes (i.e., the start time is stochastic), leading to a stochastic SGRA problem.

Let $\boldsymbol{\lambda}$ be the CIP vector containing 96-elements, where each element λ_t gives the aggregator determined CIP at time interval t. In addition to the information about the schedulable loads, the aggregator possesses information on:

- $\gamma(i, \boldsymbol{\lambda}, t)$, a binary function that represents whether the customer will allow load i to be rescheduled to time t with CIP $\boldsymbol{\lambda}$ ($\gamma = 1$) or not ($\gamma = 0$);
- $s(t)$, the forecast SMP of electricity in the bulk electricity market (in cents/kWh); and
- $r(t)$, the forecast price of electricity from the utility company (in cents/kWh).

Because the customer also has access to the forecast utility price (e.g., RTP and TOU), if the CIP, $\boldsymbol{\lambda}$, does not offer enough of a cost reduction to justify the inconvenience of rescheduling the load, the customer has the opportunity to refrain from participation, as represented by the binary function, γ (described in the customer models in Section 6.3). Therefore, the position of the aggregator is to find the following:

- L, the set of loads the aggregator is rescheduling;
- t_{i_resch}, the rescheduled start time for load i; and
- $\boldsymbol{\lambda}$, the CIP vector

to maximize profit. Let I be the total number of schedulable loads. The cardinality of L is less than or equal to I (i.e., $|L| \leq I$) because the aggregator has information about all I schedulable customer loads, but it does not necessarily have to reschedule all loads.

6.2.4 Aggregator profit function

For the aggregator, let S be the *total income received* for selling electricity to customers, given by (6.1); N be the *total income received* for selling negative load to the spot market given by (6.2); and B be the *total cost paid* to the spot market for buying electricity given by (6.3). The exact payment received from N would depend on policy, such as the outcome of FERC Order 745 [17] and its future iterations; however, we are not addressing energy policy in this chapter. We assume that the aggregator is a well-behaved agent that does not manipulate the market (such as by misrepresenting the sum of the negative load) and is paid the difference from a deterministic baseline load. The calculations for S, N, and B are given as:

$$S = \sum_{i \in L} \left[\gamma(i, \boldsymbol{\lambda}, t_{i\_resch}) \sum_{t=t_{i\_resch}}^{t_{i\_resch}+\delta_i-1} \frac{\lambda_t p_i}{4} \right] \tag{6.1}$$

$$N = \sum_{i \in L} \left[\gamma(i, \boldsymbol{\lambda}, t_{i\_resch}) \sum_{t=t_{i\_start}}^{t_{i\_start}+\delta_i-1} \frac{s(t) p_i}{4} \right] \tag{6.2}$$

$$B = \sum_{i \in L} \left[\gamma(i, \boldsymbol{\lambda}, t_{i\_resch}) \sum_{t=t_{i\_resch}}^{t_{i\_resch}+\delta_i-1} \frac{s(t) p_i}{4} \right] \tag{6.3}$$

The forecast aggregator profit P is given as:

$$P = N + S - B \tag{6.4}$$

The terms are illustrated in Figure 6.3.

6.3 Customer models

6.3.1 Customer overview: Gamma parameter

Each customer under agreement with the aggregator has a set of schedulable loads. In this chapter we are only considering flexible, non-interruptible smart appliances (e.g., clothes dryers to avoid thermal losses) according to the definitions given in Reference 18. Each customer load has an *availability window* associated with it, describing the times during the day that their schedulable load can be rescheduled by the aggregator. In addition to the availability window, each customer has an option to veto the offer from the aggregator through the use of the γ utility variable. If the customer does not feel that the offer from the aggregator is worth the added inconvenience of rescheduling a particular load, the customer can set $\gamma = 0$ for that load on a day-to-day basis.

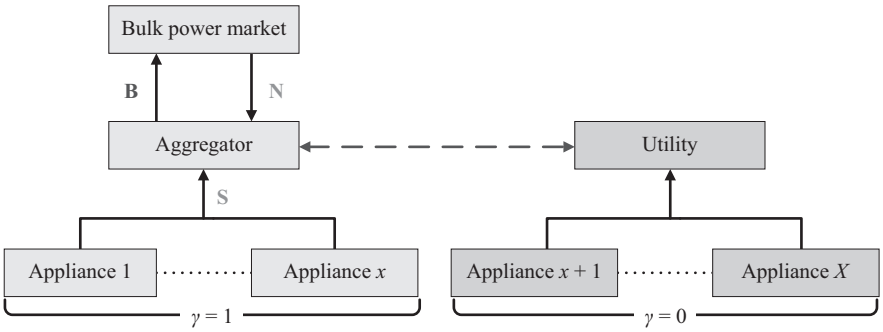

Figure 6.3 The exchange of money between the aggregator, customer, bulk power market (through the ISO), and utility. Each customer has an appliance-by-appliance choice of electricity provider. The customers of appliances {1, . . . , x} pay the customer-incentive pricing to the aggregator for use of these appliances for DR. The CIP offers for appliances {x + 1, . . . , X} were not worth the inconvenience, so those customers instead purchase electricity from the utility company for those appliances. This selection of appliances occurs on a daily basis and could be a manual choice or automated through the use of a HEMS or smart phone app. The solid arrows represent the money flowing in the system. The dashed arrow indicates the possible need for a relationship between the aggregator and utility company for use of the electrical distribution equipment

The customer sets $\gamma = 1$ to accept an offer for a particular asset. This interaction occurs on a day-by-day basis and is illustrated in Figure 6.3. This process could be automated on the customers' side, e.g., through a HEMS or smart phone app.

Only those loads that are agreed on for DR between the customer and aggregator utilize the CIP. The base load and those loads not used for DR will utilize the status quo of the utility company, e.g., RTP and TOU. This choice of supplier is a powerful new tool for the customer and offers the customer an avenue to participate in the bulk power market (through the aggregator entity), which may reduce the customer electricity bill and offers a freedom of choice of electricity supplier. Each customer has a baseline load and a set of schedulable loads, as described in Section 6.3.3. To determine the value of γ for each aggregator customer schedulable appliance, we use the alpha model described in the following section.

6.3.2 Alpha model

6.3.2.1 Alpha model overview

A key assumption in the proposed DR methods is customer participation. We model the behavior of each customer for determining whether or not they will allow the aggregator to reschedule their smart appliances using the proposed alpha-model.

In the alpha-model, each schedulable load i has an associated threshold metric for "customer comfort" in percent, α_i. Let c_{i_0} be the original cost of running load i at the utility price and c_{i_sch} be the rescheduled cost of running load i at the CIP offered by the aggregator. For the owner of load i to allow it to be rescheduled (i.e., $\gamma = 1$), the inequality $c_{i\_sch} \leq \alpha_i c_{i\_0}$ must hold. This new model allows flexibility for the customer on a load-by-load basis. Additionally, the customer is always guaranteed (if its loads are used by the aggregator), to save $1 - \alpha_i$ times the cost of running load i compared to paying the utility price. Customer inconvenience is captured through the γ value and availability window, as opposed to the time-dependent models in References 19 and 20. The customer γ values are private, and the aggregator is assumed to operate without receiving this information explicitly.

To determine α_i for simulation studies, we use three different methods: constant-α, Gaussian, and the coefficient-of-variation-based (CVB) method. The three methods are used to determine the effect of increasing amounts of variance in the α value and the impact on aggregator profit versus customer savings. The constant-α method sets $\alpha_0 = \alpha_1 = \cdots = \alpha_{I-1} = y$, where y is a user-defined constant. In the Gaussian method, the α value for each schedulable appliance is sampled from a random variable $\sim \mathcal{N}(\mu_\alpha, \sigma_\alpha)$. The CVB method is used to introduce ordered heterogeneity into the randomness, and is described in detail in the following section.

6.3.2.2 Coefficient-of-variation-based method

We use the CVB method to generate the α values for each load i, similar to generating task execution times for a heterogeneous suite of machines in a computing environment [21]. We offer an analogous method of generating load α values for a heterogeneous suite of customers. This approach is taken because it is assumed that customers will act similarly when using similar load types (e.g., more flexible with laundry, less flexible with the TV).

Let μ_a be the desired average α value for all loads, σ_a be the desired coefficient-of-variation of the load types, and σ_c be the desired coefficient-of-variation of the customers within a load type. For each load type k, we sample from a Gamma distribution with mean μ_a and standard deviation σ_a to obtain the mean α value for load type k, denoted $\mu_{a,k}$. For each customer that owns load type k, obtain α_i by sampling a Gamma distribution with mean $\mu_{a,k}$ and standard deviation σ_c. This gives similar α values for each type of load, and thus similar customer behavior.

Let $\mathcal{G}(v, \theta)$ be a Gaussian distribution with shape v and scale θ. We can define these values as functions of the mean μ and variance σ^2, given in (6.5) and (6.6), respectively. The CVB method is then provided as pseudocode in Figure 6.4.

$$v(\mu, \sigma^2) = \frac{\mu^2}{\sigma^2} \tag{6.5}$$

$$\theta(\mu, \sigma^2) = \frac{\sigma^2}{\mu} \tag{6.6}$$

A parameter sweep was performed on the input values μ_a, σ_a, and σ_c. A representative result is shown in Section 6.6 using the inputs $\mu_a = 0.75$, $\sigma_a = 0.10$, and

```
for load type k do
    μ_{a,k} = G(v(μ_a, σ_a^2), θ(μ_a, σ_a^2))
    for asset i do
        if asset i is of type k then
            α_i = G(v(μ_{a,k}, σ_c^2), θ(μ_{a,k}, σ_c^2))
        end if
    end for
end for
```

Figure 6.4 Pseudocode for the CVB method for determining asset α values

$\sigma_c = 0.05$. In general, the magnitude of the CIP is sensitive and positively correlated to μ_a (i.e., as μ_a increases, the CIP proportionally increases with respect to the RTP). Values of σ_a and σ_c are positively correlated with the noise level of the CIP.

6.3.3 Customer loads

Two types of loads are assumed to be available for each customer in this study: baseline and schedulable (smart) appliances. The baseline load is divided into thermal, modeled as air conditioning [22] and electric water heaters [12], and other non-schedulable loads. The non-schedulable loads are probabilistically generated for each customer based on the data in Reference 23.

A probabilistic model for 18 generic schedulable appliance types is given in Reference 1. The penetration level gives the probability that an appliance is present for a given customer; if it is present, the rated power of the appliance, as well as the start hour, is obtained from a normal distribution. The values probabilistically reflect the actual energy use of an average household. Similar to the non-schedulable loads, a set of schedulable loads corresponding to each customer is generated.

Each probabilistically generated load i has an associated availability window, (A_{i_start}, A_{i_dur}), that describes the time-window that the customer has allocated for load i to be scheduled. Recall that t_{i_start} is the originally scheduled starting time for load i. Let $\mathcal{U}(\delta_i, 96)$ be a uniform random variable in the interval $[\delta_i, 96]$. In our study, to generate the availability window for each load i, an interval of duration $\mathcal{U}(\delta_i, 96)$ is generated around the starting time t_{i_start}. That is, $A_{i\_dur} = \mathcal{U}(\delta_i, 96)$ and $A_{i\_start} = t_{i\_start} - \frac{A_{i\_dur}}{2}$. Other methods can be used to determine the start time and duration of a set of schedulable loads, such as an $M_t/G/\infty$ queue [24].

6.4 Pricing mechanisms

The different utility pricing mechanisms used for this chapter are a flat rate tariff, TOU, and RTP. The RTP information used in the simulation is real data from the ComEd Residential RTP program [25] from July 23, 2015, shown as the solid lines in

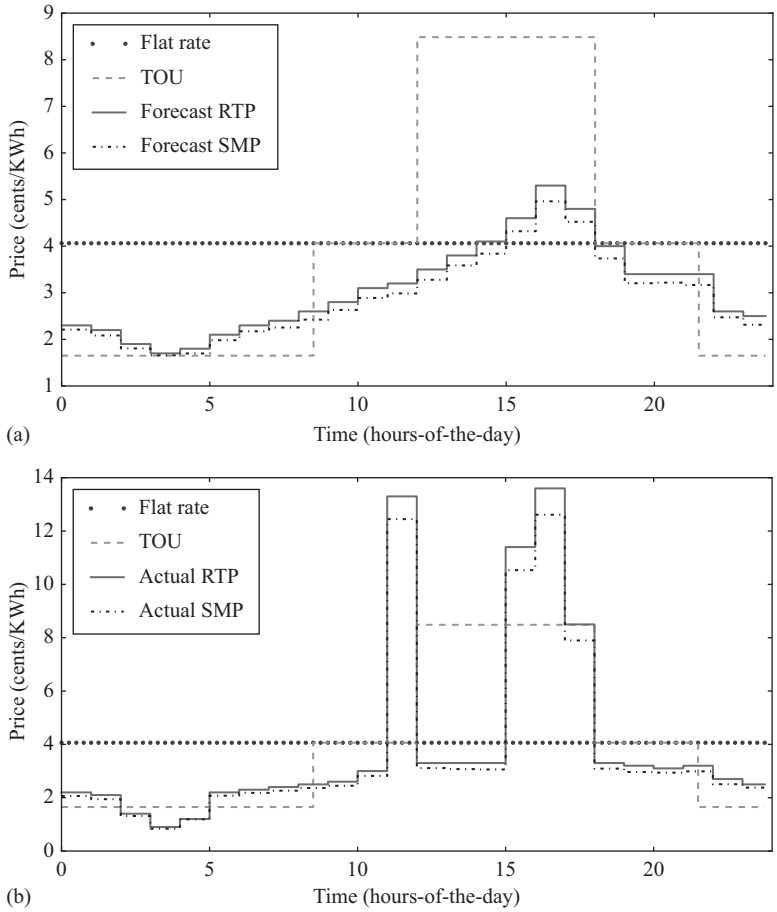

Figure 6.5 Real-time (RTP) [25] and spot market pricing (SMP) [27] from July 23, 2015, compared to flat-rate and time-of-use (TOU). (a) The day-ahead forecast prices and (b) the actual market-clearing prices. The flat-rate and TOU are the same for the day-ahead and real-time periods

Figure 6.5. The RTP market is modeled after the ComEd Residential RTP program [25]. The price of electricity changes every hour in response to the PJM real-time hourly market price. At approximately 4:30 pm, a forecast for the next day's hourly prices are provided to the customer. At the start of each hour, the actual price for that hour is provided. This data is given as 24 1-h intervals.

To make a fair comparison to the RTP, the flat rate used the mean value of the actual RTP, which was 4.06 cents/kWh. The TOU schedule was taken for the summer season from Pacific Gas and Electric (PG&E) [26], summarized in Table 6.1. The day is split into three time periods: off-peak, partial-peak, and peak, where the price

Table 6.1 Time-of-use rate periods

Period	Time	Price (cents/kWh)
Off-peak	21:30–8:30	1.65
Partial-peak	8:30–12:00, 18:00–21:30	4.06
Peak	12:00–18:00	8.48

of electricity in each subsequent period is more expensive. To determine the rates for each period to provide a fair comparison to the RTP and flat rate, the partial-peak was set at the mean price (i.e., 4.06 cents/kWh). The off-peak rate was chosen as the twenty-fifth percentile of the RTP curve, and the peak was set proportionally to keep the total mean of the TOU equivalent to the mean of the RTP and flat rate. These prices were chosen to provide a CIP comparison to the real RTP data for the day in question. The results should not be used to make general conclusions about the performance between RTP and TOU.

The aggregator also uses information about the forecast and real-time SMP in the scheduling decisions (i.e., in (6.2) and (6.3)). The SMP information used in the simulation was also real data from July 23, 2015, obtained from PJM [27]. The day-ahead forecast pricing is given in Figure 6.5(a) and the actual pricing is given in Figure 6.5(b).

6.5 Heuristic framework

6.5.1 Problem formulation

In this section, we formally define the heuristic framework in terms of the optimization function and heuristic implementation. We use heuristic optimization in this chapter because, in general, scheduling problems are NP-complete [8–10], and thus exact optimal methods are non-tractable. The heuristic optimization problem is set up as follows:

$$\max_{t_{i\_resch} \forall i \in L, \boldsymbol{\lambda} = (\lambda_0, \ldots, \lambda_{95})} \quad P \tag{6.7}$$

subject to

$$A_{i\_start} \leq t_{i\_resch} \leq A_{i\_start} + A_{i\_dur} \qquad \forall i \in L \tag{6.8}$$

and

$$t_{i\_resch} \in \mathbb{Z} \qquad \forall i \in L \tag{6.9}$$

$$\lambda_t \in \mathbb{R} \qquad t = 1, \ldots, 96 \tag{6.10}$$

$t = 0$	$t = 1$	...	$t = 95$	load_0	load_1	...	load_I
$\boldsymbol{\lambda_0}$	$\boldsymbol{\lambda}_1$	...	$\boldsymbol{\lambda}_{95}$	$t_{0,\text{sch}}$	$t_{1,\text{sch}}$	...	$t_{I,\text{sch}}$

Figure 6.6 The chromosome structure for the genetic algorithm. The genes $\lambda_0, \ldots, \lambda_{95}$ represent the customer-incentive pricing vector, one element for each 15-min interval in the 24-h period. The genes $t_{1\_sch}, \ldots, t_{I\_sch}$ are a representation of the aggregator schedule for the I customer loads that are schedulable. If the t_{i_sch} represents the original start time t_{i_start}, then the aggregator has not chosen to reschedule that appliance for use in DR

6.5.2 Genetic algorithm implementation

In this research, the steady-state Genitor [28] version of genetic algorithm (GA) is used to implement the heuristic framework. We use a GA as an example global search heuristic as GAs have been shown to work well in many optimization problems, such as resource allocation in computing [29–31], economic dispatch [32], and unit commitment [33], but any heuristic optimization method can be used to implement the described framework. If multiple objectives are used, the GA can easily be extended to generate Pareto fronts, e.g., with NSGA-II [16,34].

The implemented chromosome structure is broken into two parts, each with its own gene type, shown in Figure 6.6. The first portion of the chromosome is dedicated to the CIP vector, $\boldsymbol{\lambda}$, containing 96 genes representing the CIP (in cents/kWh) for each of the corresponding 15-min intervals of the day. The second portion of the chromosome represents the schedule of loads, containing one gene for each of the I schedulable customer loads. Let t_{i_sch} be a real value in the interval [0, 1] representing the scheduled start time of load i. The time interval that each load i is scheduled is calculated as $t_{i\_resch} = A_{i\_start} + t_{i\_sch}A_{i\_dur}$. If $t_{i\_resch} = t_{i\_start}$, then the load has not been used in DR (i.e., $i \notin L$). The [0, 1] representation of t_{i_sch} is used to avoid violating the customer-defined availability constraints of the loads given in (6.8).

No duplicate chromosomes are allowed in the initial population of Genitor to prevent premature convergence. Genitor is a steady-state algorithm that maintains a ranked list of chromosomes (in our study, ranked by (6.4)) to keep the best solutions between generations, i.e., elitism. In each generation, two parent chromosomes are selected using the linear bias function (as defined in Reference 28) to perform the global search. The linear bias selection function uses a linear bias parameter, $[1, 2] \in \mathbb{R}$, to bias selection toward the better solutions. A linear bias parameter of 1.5 means the best-ranked solution has a 50% greater chance of being selected than the median solution.

After two parent chromosomes are selected using the linear bias function, crossover and mutation search operators are performed. The former uses a two-point crossover performed separately on each of the two portions (CIP and schedule) of the chromosome. After crossover, two new children chromosomes are created. Within each child chromosome, each gene has a probability of mutation that randomly

```
initialize starting population
sort population by (6.4)
repeat
    select two parent chromosomes via linear bias
    create two children chromosomes using crossover
    mutate children genes probabilistically
    insert children chromosomes into population
    remove two worst chromosomes from population
until stopping criteria
return best chromosome from population according to (6.4)
```

Figure 6.7 Pseudocode for the steady-state Genitor algorithm

generates a new value for that gene. These new chromosomes are evaluated in terms of the objective function (given in (6.7)), inserted into the sorted population, and the worst two chromosomes in the population are removed, leading to a fixed population size. The complete algorithm is shown as pseudocode in Figure 6.7.

A parameter sweep was used to determine the best parameters to use for the GA in the scope of this problem. The population size was 100, the linear bias parameter was 1.4, and the probability of mutation was 0.01. The stopping criteria were defined as 500,000 total iterations or 10,000 iterations without an increase in the objective function.

To increase the search speed and quality of the Genitor solution, the initial population was seeded. Let ω be a real value in the interval [0, 1]. To seed the CIP vector, $\boldsymbol{\lambda}$, in 50 chromosomes in the initial population, we use the seeding function, denoted $\sigma(t, \omega)$, for each time-window $t = 1, \ldots, 96$, given by (6.11). The schedule for the customer load was randomly generated for each seed. The 50 seeds were generated using values $\omega = \frac{n}{49}$, $n = 0, \ldots, 49$.

$$\sigma(t, \omega) = \begin{cases} \omega s(t) & s(t) \geq r(t) \\ \omega r(t) & s(t) < r(t) \end{cases} \tag{6.11}$$

The rest of the chromosomes in the initial population are randomly generated. For each gene in the CIP vector, representing the cost in cents/kWh at time t, a random value is generated in the interval $[0, \max(r(t), s(t))]$. For each gene in the schedule, representing the scheduled time of load i, a random value in the interval [0, 1] is generated. The data in Figure 6.5(a) is used by the GA to determine $\boldsymbol{\lambda}$ and the schedule of loads.

6.6 Simulation study

6.6.1 Simulation setup

A total of 56,588 schedulable loads (i.e., $I = 56,588$) from the 5,555 customers were randomly generated using the method from Section 6.3.3. The schedulable customer

Table 6.2 Aggregator forecast profit (in USD)

	RTP	**TOU**	**Flat rate**
Constant-$\alpha = 0.75$	699.06	863.33	954.10
Gaussian$\sim \mathcal{N}(0.75, 0.1)$	649.78	782.79	760.51
CVB	660.48	786.87	810.59
Constant-$\alpha = 1.0$	872.34	1101.38	1272.45

loads correspond to 18.7% of the total energy used by the 5,555 customers, equivalent to 30.6 MWh. To capture the aggregator DR in steady-state, a 2-h window was added to the start and end of the simulation time. Any appliance load that occurs within these windows did not contribute toward the objective function (i.e., only the 24-h window was used for the objective function calculation). Different cases were simulated using the different pricing mechanisms from Section 6.4 and the different alpha-models in Section 6.3.2, summarized in Table 6.2. Each case used the same set of customer appliances, generated α-values (within a table row), and price (within a table column). The stopping criteria for the Genitor algorithm were 500,000 total iterations, or 10,000 iterations without an increase in the objective function of the best solution (whichever occurs first). On average across all cases, the Genitor ran for 423,813 iterations in 188 min on a Dell Server with an Intel Xeon E5-2560 running at 2.4 GHz using a C++ implementation on a Ubuntu virtual machine.[2]

6.6.2 Results

The total system load before and after the aggregator-based DR is shown in Figure 6.8(a). This result is for the CVB method for generating α values (the CVB row in Table 6.2) for each of the three utility pricing mechanisms. In all three shown cases, the aggregator was able to reduce the peak of the system by approximately 2–2.5 MW, equating to a 12.5% peak reduction. All load shapes were similar when using the other methods of generating α values. To obtain better resolution on the effect of the aggregator, the schedulable load of the system is isolated and shown in Figure 6.8(b). Here, the difference in pricing mechanisms becomes apparent. In all cases, over half of the schedulable load at the peak (around 5 pm) is moved off-peak. The reason this value is not higher is due to the customer availability windows described in Section 6.2.3. Because of this constraint, not all of the load can be moved to off-peak hours. The large negative difference in load before and after DR, especially at the peak, directly corresponds to the component of aggregator profit obtained by selling negative load, N, to the spot market. The positive difference in load (i.e., when the "after" load is higher than the "before") is the portion of the load that contributes to the $S - B$ component of the aggregator profit function.

[2]The simulation code and data sets are made available at https://github.com/IPEMS.

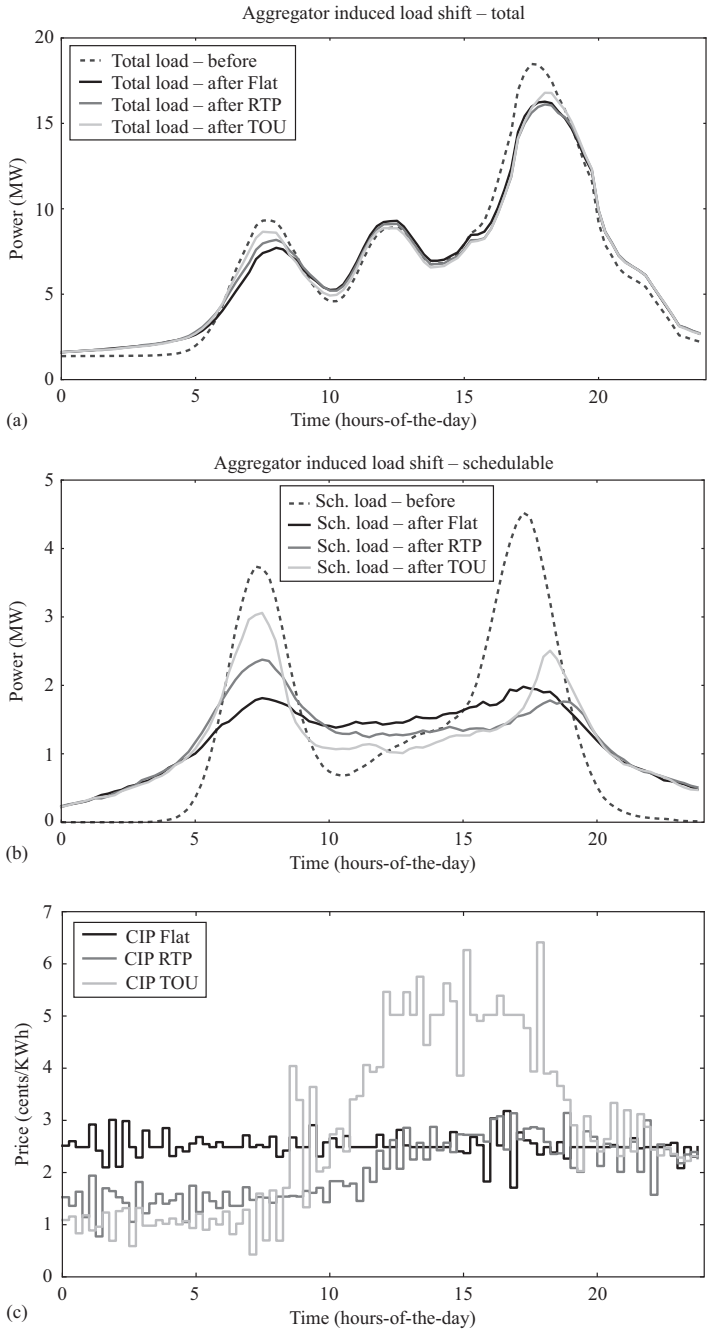

Figure 6.8 The change in load from before and after the aggregator demand response action compared to the aggregator CIP. This data is for the CVB method for generating the appliance α-values. (a) The overall system load of the 5,555 customers. (b) The schedulable load. (c) The CIP

Table 6.3 Aggregator profit after the market clears (in USD)

	RTP	**TOU**	**Flat rate**
Constant-$\alpha = 0.75$	960.53	1124.11	1135.88
Gaussian$\sim \mathcal{N}(0.75, 0.1)$	904.85	1048.19	944.89
CVB	918.02	1056.20	991.85
Constant-$\alpha = 1.0$	1102.87	1352.47	1452.05

Interesting details between the different utility pricing mechanisms emerge in Figure 6.8(b). In the TOU case, the aggregator pushes as much load as possible off of the "peak" price at the second peak load (18:00 h), and off of the "partial-peak" price at the first peak load (8:30 h). During the morning partial-peak price and peak price (8:30 am to 6:00 pm), the TOU case has the lowest schedulable load. In the flat rate case, the aggregator choice purely depends on the forecast SMP (from Figure 6.5(a)) and the schedulable load curve is flattened. The RTP case depends on the forecast SMP *and* RTP, which have very similar shapes because the ComEd utility passes the SMP to the customer with a slight markup. The forecast peak and valley of the RTP/SMP occurs at 4–5 pm and 3–4 am, respectively. As such, the aggregator tries to move as much load off of the peak RTP time as possible, and tries to move load from the morning load peak toward the price valley. The aggregator-determined CIPs for the CVB cases are shown in Figure 6.8(c). The determined CIP is always lower than the forecast prices in each utility pricing case, and the majority of the time the CIP is lower than the actual RTP. In the flat rate and TOU cases, the CIP is always lower than the utility price, indicating the customer receives a competitive, and reduced, rate of electricity for participating with the aggregator.

The final objective value, i.e., forecast aggregator profit P, for the different cases are given in Table 6.2 (based on Figure 6.5(a)). When evaluated for the *actual* RTP (for the RTP cases) and SMP, the aggregator schedule and CIP determined by the Genitor resulted in the aggregator profit given in Table 6.3 (based on Figure 6.5(b)). This increase in profit from forecast to actual is because the actual SMP at the peak period was much higher than forecast (as shown in Figure 6.5), leading to an increase in profit from the N component (6.2) of the profit function.

In each case, the constant-α values of 0.75 and 1.0 (denoted C75 and C100, respectively) allowed the aggregator to make the most profit. This is because the GA was able to find CIPs close to the optimal solutions in these cases – a CIP of 75% and 100% of the utility rate in the C75 and C100 cases, respectively – compared to the other alpha methods. The CIPs for C100 and C75 are shown in Figure 6.9(a) and (b), respectively. This is most obvious in the CIPs for the flat rate and TOU in the C100 case in Figure 6.9(a). The CIP flat rate curve found by the GA is very close to the utility flat rate of 4.06 cents/kWh, shown in Figure 6.5. Similarly, the partial-peak and peak values for the CIP TOU case are very similar to the utility TOU price. The same trend can be found in Figure 6.9(b) for the C75 case, but the CIP values are near 75%

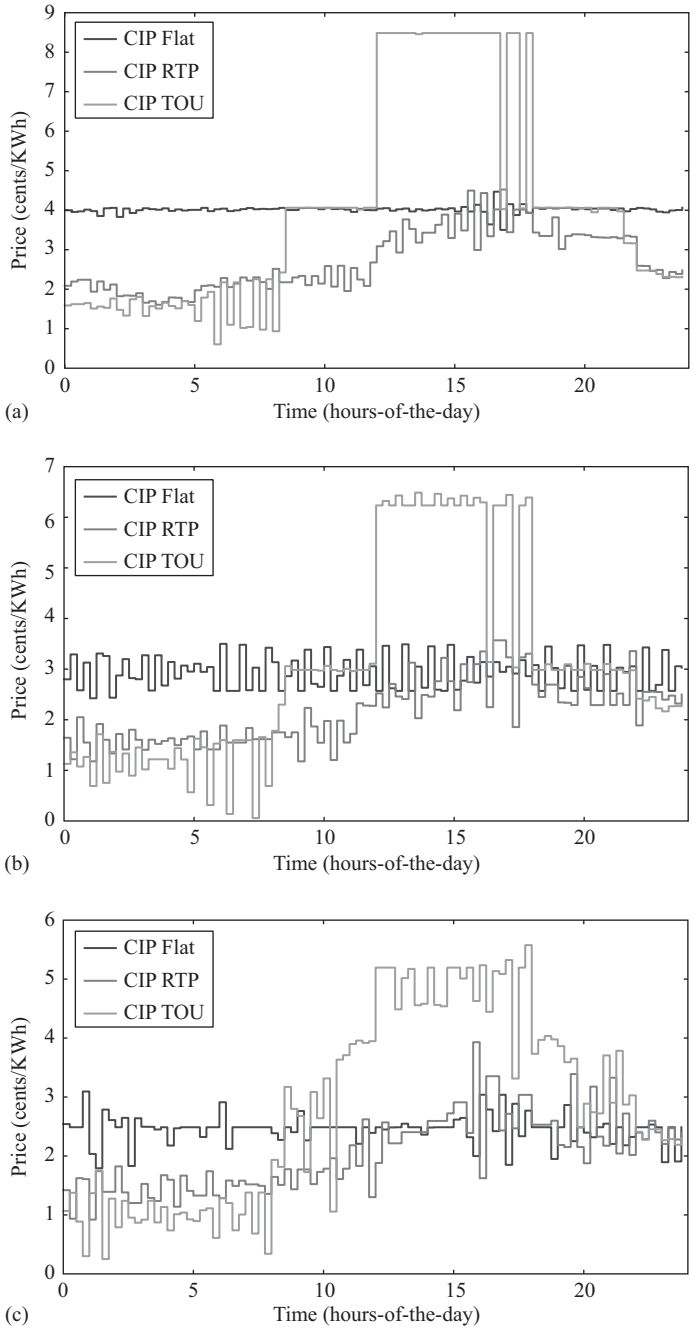

Figure 6.9 A comparison between the utility pricing mechanisms of the aggregator-determined CIPs for the (a) constant-$\alpha = 1.0$, (b) constant-$\alpha = 0.75$, and (c) Gaussian$\sim \mathcal{N}(0.75, 0.1)$ cases. The CVB case is provided in Figure 6.8(c)

Table 6.4 Forecast total customer savings (in USD)

	RTP	**TOU**	**Flat rate**
Constant-$\alpha = 0.75$	400.62	606.59	326.15
Gaussian$\sim \mathcal{N}(0.75, 0.1)$	414.12	658.00	429.78
CVB	426.66	665.63	436.93
Constant-$\alpha = 1.0$	244.95	360.28	12.88

of those in the utility pricing cases. The C100 case is most likely unrealistic as the customer is giving up the convenience of their loads for no monetary benefit, as shown in Table 6.4, and is used as a pseudo-upper-bound on the profit of the aggregator.[3]

In all alpha models, the RTP pricing is the worst performing in terms of aggregator forecast profit and actual aggregator profit. This could be due to the difficulty in the search space for finding the correct CIP, but also because loads that run greater than 1 h (or cross the hourly boundary during their duration) will cost two separate prices per kWh. This makes it difficult for the aggregator to schedule many long-running appliances from many customers at a significant profit. In general, for the results from this single day study, the aggregator made the most profit, in descending order of profit, for flat rate, TOU, and RTP; and in terms of customer alpha models for constant-α, CVB, and Gaussian (Tables 6.2 and 6.3). The significant differences in pricing methods and aggregator profit could be due to the method used for determining the values of the flat rate and TOU price in Section 6.4. For example, a weighted average of the price compared to the peak load may have resulted in a different mean value for price (i.e., the flat rate price and the partial-peak price of TOU). Additionally, the choice of 25% for the TOU off-peak price could be changed to any value and would impact the results. As these results are for a single sampling of the α-values for the stochastic Gaussian and CVB methods for a single day, no general conclusion can be made for the relative performance of the two methods without conducting simulations to estimate their statistical performance.

From a customer perspective, the total savings of all 5,555 customers are given in Tables 6.4 and 6.5 when using the forecast and actual data, respectively, for the 24-h period under consideration. An increase in savings similar to the aggregator's increase in profit is found in the RTP case, due to the large increase in peak RTP that the customer choosing CIP no longer has to pay. For the TOU and flat rate cases, there is no difference in forecast and actual savings because there is no uncertainty in the price of electricity for the customer. As a customer, participating with the aggregator in the TOU and flat rate cases provides a guaranteed, known benefit. When participating with the aggregator in the RTP case, the customer is offered stability in the price of electricity as the aggregator CIP is guaranteed the day-ahead.

[3]Monetary benefits may not be the only consideration for early adopters of new technology. Instead, some customers are motivated by altruistic reasons, such as environmental benefits (i.e., "being green") [35].

Table 6.5 Actual total customer savings (in USD)

	RTP	TOU	Flat rate
Constant-$\alpha = 0.75$	972.93	606.59	326.15
Gaussian$\sim \mathcal{N}(0.75, 0.1)$	983.32	658.00	429.78
CVB	1002.27	665.63	436.93
Constant-$\alpha = 1.0$	819.32	360.28	12.88

Table 6.6 Percent of rescheduled loads

	RTP (%)	TOU (%)	Flat rate (%)
Constant-$\alpha = 0.75$	83.4	72.6	94.9
Gaussian$\sim \mathcal{N}(0.75, 0.1)$	80.6	70.3	87.8
CVB	82.7	71.3	92.6
Constant-$\alpha = 1.0$	86.1	73.0	95.4

The CVB method is consistently the highest performing in terms of customer savings, which is a promising result as it is the closest to actual human behavior. By assigning similar appliances similar α-values (through the setting of the $\mu_{a,k}$ for appliance type k), the aggregator-determined CIP and schedule benefits the average customer. In the best case (CVB and RTP), the average customer saved \$0.18. Although this is for a single day, a rough extrapolation of this value would save the customer around \$5.50 per month. In general, the aggregator makes less profit and the customer saves more when the average α-value is decreased, and vice versa.

The maximum customer savings from all cases was \$0.51. This customer had an average $A_{i\_dur} > 15$ h on 12 loads with a total energy of 92.9 kWh. The average alpha value for this customer was $\alpha = 0.76$. Using the same extrapolation estimate, this customer, for being flexible with the loads, could save between \$15 and \$16 per month, which is a large percentage of the monthly bill. This is indicative of the possible monetary benefits from the customer being more flexible with loads (in the availability of the reschedulable load and the customer α-values) and bringing more energy (i.e., an asset set with a large kWh rating) to the aggregator to participate in DR.

In Table 6.6, the percent of reschedulable loads that the aggregator utilized in DR is provided (i.e., $^{|L|}/_{I}$). It is interesting to note that even though the TOU was the second best performing algorithm in terms of aggregator profit in most cases (some cases it performed the best), and had the highest *forecast* customer savings, TOU had the least number of rescheduled loads. This occurs because the TOU has relatively long periods of constant price, and the difference between the price periods is relatively large. This allows the aggregator to shift load in small time displacements and receive large rewards for both the customer and the aggregator. This becomes more apparent in the heat maps in Figure 6.10, specifically in Figure 6.10(b).

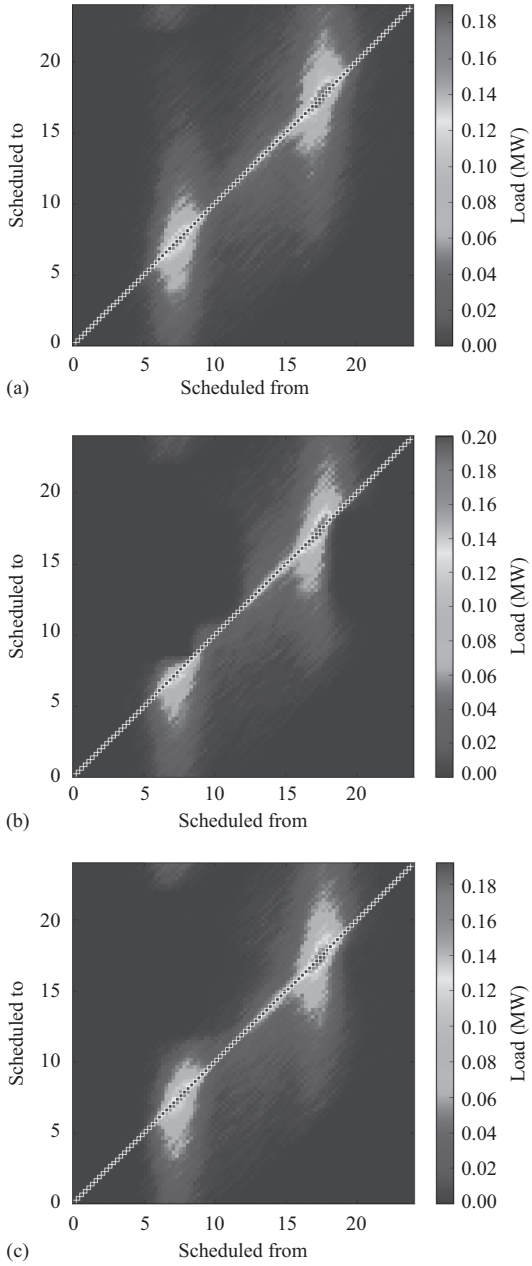

Figure 6.10 *Heat maps for the rescheduled load in the CVB alpha model case for the (a) flat rate, (b) TOU, and (c) RTP utility pricing mechanisms. For each (x, y) coordinate, the color of the square in the heat map indicates the magnitude of the load that was rescheduled from time x ($t_{i\_start} = x$) to time y ($t_{i\_resch} = y$)*

To further characterize the impact of the aggregator-based residential DR program, for Figure 6.10 we use the heat map visualization methods from Reference 36. For each (x, y) coordinate, the color of the square in the heat map indicates the magnitude of the load that was rescheduled from time x ($t_{i\_start} = x$) to time y ($t_{i\_resch} = y$). For $x > y$ (i.e., below the diagonal), the plot indicates the load was scheduled earlier, and $x < y$ indicates the load was scheduled at a later time. At a $t_{i\_start} = x$, the larger the value of $|y - x|$, the further away the load was scheduled by the aggregator DR. This distance is limited by the customer defined availability window. The heat maps only show the load that was rescheduled. The load that was not rescheduled (i.e., $\notin I$) would appear on the diagonal ($x = y$), but for visualization purposes it is set to 0 MW. We do this because the magnitude of the load that is not scheduled is much larger than any individual (x, y) magnitude where $x \neq y$, reducing the resolution of the interesting portions of the heat map. The flat rate, TOU, and RTP cases for the CVB alpha model are shown in Figure 6.10(a)–(c), respectively. The flat rate and RTP cases are very similar, except the flat rate case schedules the loads from the first peak to a much later time than the RTP. This can be seen in the verticality of the loads near 8:00 am between the two heat maps, i.e., the loads scheduled *from* the times around 8:00 am are rescheduled *to* more times in the y-direction. The magnitude of the two heat maps are very similar, but there is much more load rescheduled in the flat rate case (as was shown in Table 6.6). In the TOU case, it is very interesting to see how the aggregator schedules load around the change in price periods. The aggregator in the TOU case does not schedule load *to* the partial-peak price in the morning, shown as the horizontal flat transition at $y = 8{:}30$ between $5{:}00 < x < 10{:}00$. Similarly, the aggregator does not schedule load *from* the partial-peak price in the evening, shown as the vertical flat transition at $x = 18{:}00$.

6.7 Conclusions

We presented an aggregator-based residential DR approach for scheduling residential customer assets. A CIP structure to compensate the customer for the inconvenience of rescheduling their assets is discussed and compared to three utility rate structures. This new pricing structure gives the customer a near real-time choice of electricity supplier in a fully deregulated market scenario. A heuristic framework was designed to perform an optimization on the profit of the aggregator. To validate the heuristic framework, a system comprised 5,555 customer households and 56,588 schedulable loads was simulated using a GA implementation of the framework. The CIP found by the GA was, in general, lower at all times than the customer would pay via all forms of real utility pricing data (or with reasonable modifications), i.e., RTP, TOU, and flat rate tariff for a given day in summer 2015. Despite this, the aggregator was able to make a profit by selling negative peak load to the spot market. This showed an example of optimizing for purely economical reasons in the form of aggregator profit, and enacting an overall change on the system peak load. This change benefits the customers of the aggregator (in the form of reduced cost of electricity for schedulable loads), the aggregator (in the form of a profit), and also those customers

not participating with the aggregator (because the overall system peak is lowered as a common good).

Reducing the peak demand of the electric power system provides benefits by reducing the cost of electricity by lowering the deployment of expensive generators during peak hours. By reducing the peak, we can reduce the capacity factor of dirty diesel-fired peaking generators. Moreover, as peak demand increases, the available transmission capacity will also need to increase. By reducing the peak demand, we can defer building new transmission lines; a costly, long-term project. As more asset types with more capabilities, such as electric vehicles and HVAC, are considered in similar studies, the savings can be expected to increase.

References

[1] T. M. Hansen, R. Roche, S. Suryanarayanan, A. A. Maciejewski, and H. J. Siegel, "Heuristic optimization for an aggregator-based resource allocation in the Smart Grid," *IEEE Transactions on Smart Grid*, Jul. 2015, vol. 6, no. 4, pp. 1785–1794.

[2] United States Department of Energy, "The Smart Grid: An introduction," 2009. [online]. Available: http://energy.gov/oe/downloads/smart-grid-introduction-0

[3] P. Siano, "Demand response and smart grids—A survey," *Renewable and Sustainable Energy Reviews*, Feb. 2014, vol. 30, pp. 461–478.

[4] A. Zipperer, P. Aloise-Young, and S. Suryanarayanan, "On the design of a survey for reconciling consumer behaviors with demand response in the smart home," in *North American Power Symposium (NAPS), 2013*, Sep. 2013, p. 6.

[5] P. C. Stern, "Information, incentives, and proenvironmental consumer behavior," *Journal of Consumer Policy*, Dec. 1999, vol. 22, no. 4, pp. 461–478.

[6] M. H. Albadi and E. El-Saadany, "A summary of demand response in electricity markets," *Electric Power Systems Research*, 2008, vol. 78, no. 11, pp. 1989–1996.

[7] PJM Forward Market Operations, "PJM Manual 11: Energy & Ancillary Services Market Operations, Revision 83," July 2016. [online]. Available: http://www.pjm.com/~/media/documents/manuals/m11.ashx. Accessed: Aug. 24, 2016.

[8] E. G. Coffman, *Computer and Job-Shop Scheduling Theory*. John Wiley & Sons, New York, NY, 1976.

[9] D. Fernandez-Baca, "Allocating modules to processors in a distributed system," *IEEE Transactions on Software Engineering*, Nov. 1989, vol. 15, no. 11, pp. 1427–1436.

[10] O. Ibarra and C. E. Kim, "Heuristic algorithms for scheduling independent tasks on nonidentical processors," *Journal of the ACM*, Apr. 1977, vol. 24, no. 2, pp. 280–289.

[11] California Energy Commission. "2013 Integrated Energy Policy Report." Accessed: Mar. 28, 2014. [Online]. Available: http://www.energy.ca.gov/2013_energypolicy/

[12] P. Du and N. Lu, "Appliance commitment for household load scheduling," *IEEE Transactions on Smart Grid*, Jun. 2011, vol. 2, no. 2, pp. 411–419.

[13] K. F. Fong, V. I. Hanby, and T. T. Chow, "HVAC system optimization for energy management by evolutionary programming," *Energy and Buildings*, Mar. 2006, vol. 38, no. 3, pp. 220–231.

[14] E. Sortomme and M. A. El-Sharkawi, "Optimal scheduling of vehicle-to-grid energy and ancillary services," *IEEE Transactions on Smart Grid*, Mar. 2012, vol. 3, no. 1, pp. 351–359.

[15] M. A. A. Pedrasa, T. D. Spooner, and I. F. MacGill, "Coordinated scheduling of residential distributed energy resources to optimize smart home energy services," *IEEE Transactions on Smart Grid*, Sep. 2010, vol. 1, no. 2, pp. 134–143.

[16] R. Friese, T. Brinks, C. Oliver, A. A. Maciejewski, and H. J. Siegel, "Analyzing the trade-offs between minimizing makespan and minimizing energy consumption in a heterogeneous resource allocation problem," in *2nd International Conference on Advanced Communications and Computation*, Oct. 2012, pp. 81–89.

[17] United States Federal Energy Regulatory Commission, "FERC Order 745: demand response compensation in organized wholesale energy markets," Mar. 2011.

[18] Z. Chen, L. Wu, and Y. Fu, "Real-time price-based demand response management for residential appliances via stochastic optimization and robust optimization," *IEEE Transactions on Smart Grid*, Dec. 2012, vol. 3, no. 4, pp. 1822–1831.

[19] L. Gkatzikis, T. Salonidis, N. Hegde, and L. Massoulié, "Electricity markets meet the home through demand response," in *IEEE Conference on Decision and Control*, Dec. 2012, pp. 5846–5851.

[20] T. Bapat, N. Sengupta, S. K. Ghai, V. Arya, Y. B. Shrinivasan, and D. Seetharam, "User-sensitive scheduling of home appliances," in *ACM SIGCOMM Workshop on Green Networking*, Aug. 2011, pp. 43–48.

[21] S. Ali, H. J. Siegel, M. Maheswaran, D. Hengsen, and S. Ali, "Representing task and machine heterogeneities for heterogeneous computing systems," *Tamkang Journal of Science and Engineering,* Special Tamkang University 50th Anniversary Issue, Nov. 2000, vol. 3, no. 3, pp. 195–208. Invited.

[22] N. Lu and Y. Zhang, "Design considerations of a centralized load controller using thermostatically controlled appliances for continuous regulation reserves," *IEEE Transactions on Smart Grid*, Jun. 2013, vol. 4, no. 2, pp. 914–921.

[23] R. Roche, "Agent-based architectures and algorithms for energy management in smart grids." PhD dissertation. Université de Technologie de Belfort-Montbéliard, Belfort, France, Dec. 2012.

[24] T. M. Hansen, E. K. P. Chong, S. Suryanarayanan, A. A. Maciejewski, and H. J. Siegel, "A partially observable Markov decision process approach to customer home energy management systems," http://www.engr.colostate.edu/sgra, in press.

[25] ComEd. "ComEd residential real-time pricing program." Accessed: Aug. 18, 2013. [Online]. Available: https://rrtp.comed.com/live-prices/

[26] Pacific Gas and Electric. "PG&E time-of-use rates." Accessed: Mar. 21, 2016. [Online]. Available: http://www.pge.com/TOU

[27] United States Federal Energy Regulatory Commission. "PJM daily report archives." Accessed: Jan. 14, 2014. [Online]. Available: http://www.ferc.gov/market-oversight/mkt-electric/pjm/pjm-iso-archives.asp

[28] D. Whitley, "The GENITOR algorithm and selective pressure: why rank-based allocation of reproductive trials is best," in *3rd International Conference on Genetic Algorithms*, Jun. 1989, pp. 116–121.

[29] L. D. Briceño, H. J. Siegel, A. A. Maciejewski, *et al.*, "Heuristics for robust resource allocation of satellite weather data processing on a heterogeneous parallel system," *IEEE Transactions on Parallel and Distributed Systems*, Nov. 2011, vol. 22, no. 11, pp. 1780–1787.

[30] T. D. Braun, H. J. Siegel, N. Beck, *et al.*, "A comparison of eleven static heuristics for mapping a class of independent tasks onto heterogeneous distributed computing systems," *Journal of Parallel and Distributed Computing*, Jun. 2001, vol. 61, no. 6, pp. 810–837.

[31] F. D. Croce, R. Tadei, and G. Volta, "A genetic algorithm for the job shop problem," *Computers and Operations Research*, Jan. 1995, vol. 22, no. 1, pp. 15–24.

[32] D. C. Walters and G. B. Sheble, "Genetic algorithm solution of economic dispatch with valve point loading," *IEEE Transactions on Power Systems*, Aug. 1993, vol. 8, no. 3, pp. 1325–1332.

[33] S. A. Kazarlis, A. G. Bakirtzis, and V. Petridis, "A genetic algorithm solution to the unit commitment problem," *IEEE Transactions on Power Systems*, Feb. 1996, vol. 11, no. 1, pp. 83–92.

[34] D. Kalyanmoy, A. Pratap, S. Agarwal, and T. A. M. T. Meyarivan, "A fast and elitist multiobjective genetic algorithm: NSGA-II," *IEEE Transactions on Evolutionary Computation*, Apr. 2002, vol. 6, no. 2, pp. 182–197.

[35] A. Zipperer, P. A. Aloise-Young, S. Suryanarayanan, *et al.*, "Electric energy management in the smart home: Perspectives on enabling technologies and consumer behavior," *Proceedings of the IEEE*, Aug. 2013, vol. 101, no. 11, pp. 2397–2408.

[36] T. Hansen, S. Suryanarayanan, A. A. Maciejewski, H. J. Siegel, and A. V. Modali, "A visualization aid for demand response studies in the Smart Grid," *The Electricity Journal*, Apr. 2015, vol. 28, no. 3, pp. 100–111.